A Thermostat for Molecular Dynamics of Complex Fluids

Michael P Allen, Friederike Schmid

Molecular Simulation
Journal of
Experimental Nanoscience

Taylor & Francis
Taylor & Francis Group

A Thermostat for Molecular Dynamics of Complex Fluids

Journal:	*Molecular Simulation/Journal of Experimental Nanoscience*
Manuscript ID:	GMOS-2006-0112
Journal:	Molecular Simulation
Date Submitted by the Author:	23-Jun-2006
Complete List of Authors:	Allen, Michael; University of Warwick, Department of Physics Schmid, Friederike; Universität Bielefeld, Fakultät für Physik
Keywords:	Thermostat, Canonical Ensemble, Dissipative Particle Dynamics, Nonequilibrium Molecular Dynamics, Nosé-Hoover

Molecular Simulation, Vol. 00, No. 00, DD Month 200x, 1–10

A Thermostat for Molecular Dynamics of Complex Fluids

Michael P. Allen *
Department of Physics and Centre for Scientific Computing
University of Warwick, Coventry CV4 7AL, United Kingdom

Friederike Schmid
Fakultät für Physik, Universität Bielefeld, D-33615 Bielefeld, Germany
(*Received 00 Month 200x; In final form 00 Month 200x*)

A thermostat of the Nosé-Hoover type, based on relative velocities and a local definition of the temperature, is presented. The thermostat is momentum-conserving and Galilean-invariant, which should make it suitable for use in Dissipative Particle Dynamics simulations, as well as nonequilibrium molecular dynamics simulations.

Keywords: Thermostat; Canonical Ensemble; Dissipative Particle Dynamics; Nonequilibrium Molecular Dynamics; Nosé-Hoover; Galilean-Invariant.

1 Introduction

The original papers of Nosé [1, 2] provided a new perspective on the generation of statistical ensembles by dynamical simulation. They showed that a deterministic set of equations of motion, involving just one or two extra degrees of freedom, can sample configurations from the canonical ensemble. This complements the stochastic method of Andersen [3], which generates the canonical ensemble by periodic reselection of velocities from the Maxwell-Boltzmann distribution. The work of Hoover [4, 5] further clarified the nature of the isothermal dynamical equations and how to derive them (see also the contribution of Hoover to these proceedings). The Nosé-Hoover equations incorporate a dynamical friction coefficient, whose fluctuations are driven by the difference between the instantaneous kinetic temperature (defined through the sum of squares of particle velocities) and the desired temperature.

This paper presents a new thermostat of the Nosé-Hoover type, based on an instantaneous temperature which is calculated as a weighted sum of squares of relative velocities of atom pairs. The frictional term in the equations of motion also enters in pairwise fashion, conserving momentum, and making the dynamics invariant to a Galilean transformation of velocities. There are two areas in which such a thermostat may be useful. The first area is nonequilibrium molecular dynamics (NEMD). With a conventional Nosé-Hoover thermostat, it is necessary to apply the friction term to the *peculiar* velocities of the particles, i.e. the difference between the true velocities and the local streaming velocity of the fluid at the particle positions. Failure to do this can lead to unphysical (thermostat-induced) behaviour [6] such as the stabilisation of string phases [7, 8] or the generation of steady-state antisymmetric stress [9]. One solution to these problems is to use a profile-unbiased thermostat, which requires a self-consistent determination of the streaming velocity in the course of the simulation [7–9]. A thermostat based on the relative velocities of nearby pairs of atoms may avoid, or at least ameliorate, the problem. The second area of application of the pairwise thermostat is dissipative particle dynamics (DPD). Here, in order to preserve hydrodynamic behaviour, it is essential for any thermostat to conserve momentum, and a pairwise form is one way of achieving this. This paper concentrates on the DPD case, since the suggestion of using a pairwise Nosé-Hoover thermostat was first made in this context by Stoyanov and Groot [10]. However, it should be borne in mind that the thermostat may be applied equally well to, e.g. Lennard-Jones fluids.

*Corresponding author. E-mail: m.p.allen@warwick.ac.uk

ISSN 0892-7022 print/ISSN 1029-0435 online © 200x Taylor & Francis
http://www.tandf.co.uk/journals
DOI: 10.1080/0892702YYxxxxxxxx

The paper is organised as follows. Section 2 contains a brief summary of DPD, concentrating on the temperature control aspects. Section 3 derives the equations of motion for the pairwise Nosé-Hoover thermostat, and also summarizes the equations for a thermostat based on the configurational temperature, due to Braga and Travis [11], for comparison. Section 4 presents the results of some preliminary tests for DPD simulations. Finally, section 5 contains the conclusions.

2 Dissipative Particle Dynamics

DPD [12, 13] has become a popular tool for simulating the behaviour of both simple and complex fluids. It consists of the solution of the classical equations of motion for a system of interacting particles, together with a set of stochastic and dissipative forces which control the temperature and allow one to choose the viscosity. For a simple fluid the equations may be written [12–14]

$$\dot{\boldsymbol{r}}_i = \boldsymbol{v}_i = \boldsymbol{p}_i/m_i \tag{1a}$$

$$\dot{\boldsymbol{p}}_i = \boldsymbol{f}_i(\boldsymbol{r}) - \xi \boldsymbol{V}_i(\boldsymbol{r},\boldsymbol{p}) + \sigma \boldsymbol{R}_i(\boldsymbol{r},\boldsymbol{p}) \ , \tag{1b}$$

where $\boldsymbol{r}$ and $\boldsymbol{p}$ stand for the complete set of coordinates and momenta. The so-called conservative forces $\boldsymbol{f}_i$ are derived from a pair-potential term in the Hamiltonian $\boldsymbol{f}_i = -(\partial H/\partial \boldsymbol{r}_i)$ and so may be written as $\boldsymbol{f}_i = \sum_{j\neq i} \boldsymbol{f}_{ij}$, with $\boldsymbol{f}_{ji} = -\boldsymbol{f}_{ij}$. In DPD these pair forces usually take the form

$$\boldsymbol{f}_{ij} = \alpha \boldsymbol{w}_{ij} = \alpha \boldsymbol{w}(\boldsymbol{r}_{ij}) \ , \qquad \text{with} \qquad \boldsymbol{w}(\boldsymbol{r}) = w(r)\hat{\boldsymbol{r}} \tag{2a}$$

$$\text{and} \quad w(r) = \begin{cases} (1 - r/r_{\rm c}) & r \leq r_{\rm c} \\ 0 & r > r_{\rm c} \end{cases} \ . \tag{2b}$$

Here $\boldsymbol{r}_{ij} = \boldsymbol{r}_i - \boldsymbol{r}_j$, $r = |\boldsymbol{r}|$, $\hat{\boldsymbol{r}} = \boldsymbol{r}/r$. The parameter α determines the strength of the conservative interactions, and $r_{\rm c}$ is the cutoff.

The dissipative forces $-\xi \boldsymbol{V}_i$ are also written in pairwise fashion $\boldsymbol{V}_i = \sum_{j\neq i} \boldsymbol{V}_{ij}$ with $\boldsymbol{V}_{ji} = -\boldsymbol{V}_{ij}$, usually defined thus:

$$\boldsymbol{V}_{ij} = \big(\boldsymbol{v}_{ij} \cdot \boldsymbol{w}_{ij}\big)\boldsymbol{w}_{ij} = w(r_{ij})^2 \big(\boldsymbol{v}_{ij} \cdot \hat{\boldsymbol{r}}_{ij}\big)\hat{\boldsymbol{r}}_{ij} \tag{3}$$

where $\boldsymbol{v}_{ij} = \boldsymbol{v}_i - \boldsymbol{v}_j$. A choice has been made here to use the same weighting function $\boldsymbol{w}(\boldsymbol{r})$ as in the specification of conservative forces. $\sigma \boldsymbol{R}_i$ is short for the random "forces", which also act between pairs, with a weight function $\boldsymbol{w}(\boldsymbol{r})$; the strength parameter σ is related through the fluctuation-dissipation theorem to the friction coefficient ξ and the temperature $k_{\rm B}T$ (see [12–14] for more details). The pairwise nature of all these forces guarantees the momentum conservation necessary to ensure hydrodynamic behaviour: in other words, the dynamics is Galilean-invariant. The particles represent fluid regions, rather than individual atoms and molecules: the softness and simplicity of the interactions permit the use of a long time step, compared with conventional molecular dynamics. This, and the acceleration of physical processes compared with those seen in more realistic simulations, gives an advantage of several orders of magnitude, at the cost of a very rough mapping onto specific molecular properties.

A slightly more general view of DPD treats it as conventional molecular dynamics using soft potentials, supplemented by a momentum-conserving thermostat which acts between pairs. Lowe [15] takes this approach, rather than solving the above equations. Instead, each timestep Δt involves the following operations.

(i) Positions and momenta are advanced using $\dot{\boldsymbol{r}}_i = \boldsymbol{p}_i/m_i$, $\dot{\boldsymbol{p}}_i = \boldsymbol{f}_i$.
(ii) Every pair ij (in random order, and possibly subject to a distance dependent weight or range function) is examined and, with probability $P = \nu \Delta t$, the momenta are updated: $\boldsymbol{p}_i := \boldsymbol{p}_i + \Delta \boldsymbol{p}_{ij}$, $\boldsymbol{p}_j := \boldsymbol{p}_j - \Delta \boldsymbol{p}_{ij}$,

with

$$\Delta \boldsymbol{p}_{ij} = m_{ij}\left[\zeta\sqrt{k_{\mathrm{B}}T/m_{ij}} - (\boldsymbol{v}_{ij}\cdot\hat{\boldsymbol{r}}_{ij})\right]\hat{\boldsymbol{r}}_{ij}$$

where ζ is picked from a Gaussian distribution with zero mean and unit variance, and $m_{ij} = m_i m_j/(m_i+m_j)$.

This procedure periodically reselects the component of the relative velocity along $\hat{\boldsymbol{r}}_{ij}$ from the Maxwell-Boltzmann distribution corresponding to reduced mass m_{ij}. The key parameter is the stochastic randomization frequency ν: high values of ν give effective temperature control, but also a high viscosity; low values give very weak temperature control while allowing the viscosity to be low. The thermostat is closely related to the one originally proposed by Andersen [3].

Recently, Stoyanov and Groot [10] have proposed a modification of the above method: the fraction $(1-P)$ of pairs which do not have their relative velocities stochastically updated, are instead thermalized by a deterministic method. For each such pair, a dissipative force is calculated and used to correct the momenta during the deterministic part of the step, incorporating a temperature-dependent controlling factor. Finally, the Lowe velocity reselection process is applied to the remaining fraction P of pairs as before. The idea of Stoyanov and Groot is to give more control over the separate effects of thermalization, namely temperature control and changing viscosity. Stoyanov and Groot [10] call the deterministic part of their thermostat "Nosé-Hoover", but actually it is not of this form, and has not been shown to generate the canonical ensemble. It may be noted that an algorithm resembling that of Nosé and Hoover was also described by Besold and Mouritsen [16].

3 Pairwise Nosé-Hoover Thermostat

3.1 *Derivation of Equations of Motion*

The purpose of this paper is to present a Galilean-invariant thermostat of the Nosé-Hoover type, which generates the canonical ensemble. The derivation is a straightforward implementation of the approach of Hoover [5], and a special case of the generalized Nosé-Hoover equations discussed by Kusnezov et al. [17] and Martyna et al. [18]. The result is assumed to be of the form

$$\dot{\boldsymbol{r}}_i = \boldsymbol{p}_i/m_i \tag{4a}$$

$$\dot{\boldsymbol{p}}_i = \boldsymbol{f}_i(\boldsymbol{r}) - \xi \boldsymbol{V}_i(\boldsymbol{r},\boldsymbol{p}) \tag{4b}$$

$$\dot{\xi} = G_\xi(\boldsymbol{r},\boldsymbol{p}) \tag{4c}$$

with the $\boldsymbol{V}_i(\boldsymbol{r},\boldsymbol{p})$ given by eqn (3). Eqns (4a) and (4b) are written down by analogy with eqns (1). The random forces are dropped, the friction coefficient ξ is now an additional *dynamical* variable, and the right-hand side of eqn (4c) is the object of the derivation. This is obtained from the generalized Liouville equation for the (stationary) phase space distribution function $\varrho(\boldsymbol{r},\boldsymbol{p},\xi)$

$$\sum_i \frac{\partial}{\partial \boldsymbol{r}_i}\cdot\left(\rho\dot{\boldsymbol{r}}_i\right) + \sum_i \frac{\partial}{\partial \boldsymbol{p}_i}\cdot\left(\rho\dot{\boldsymbol{p}}_i\right) + \frac{\partial}{\partial\xi}\left(\rho\dot{\xi}\right) = 0\,. \tag{5}$$

The ansatz is made that $G_\xi(\boldsymbol{r},\boldsymbol{p})$ in eqn (4c) depends only on positions and momenta, so $\partial\dot{\xi}/\partial\xi = 0$. Direct substitution shows that equation (5) is satisfied by the product form

$$\rho(\boldsymbol{r},\boldsymbol{p},\xi) \propto \exp\{-H(\boldsymbol{r},\boldsymbol{p})/k_{\mathrm{B}}T\}\exp\{-\tfrac{1}{2}Q_\xi\xi^2/k_{\mathrm{B}}T\}$$

where Q_ξ is an arbitrary constant, provided

$$\begin{aligned} G_\xi(\boldsymbol{r},\boldsymbol{p}) &= Q_\xi^{-1}\sum_i\left(\frac{\boldsymbol{p}_i}{m_i}\cdot\boldsymbol{V}_i - k_{\rm B}T\frac{\partial}{\partial\boldsymbol{p}_i}\cdot\boldsymbol{V}_i\right) \\ &= Q_\xi^{-1}\sum_i\sum_{j\neq i}\left(\boldsymbol{v}_i\cdot\boldsymbol{V}_{ij} - (k_{\rm B}T/m_i)w(r_{ij})^2\right) \\ &= Q_\xi^{-1}\sum_i\sum_{j<i}\left(\boldsymbol{v}_{ij}\cdot\boldsymbol{V}_{ij} - (k_{\rm B}T/m_{ij})w(r_{ij})^2\right) \\ &= Q_\xi^{-1}\sum_i\sum_{j<i} w(r_{ij})^2\left[\left(\boldsymbol{v}_{ij}\cdot\hat{\boldsymbol{r}}_{ij}\right)^2 - k_{\rm B}T/m_{ij}\right]. \end{aligned} \tag{6}$$

Once more, the reduced mass m_{ij} appears. The term in square brackets vanishes if an average is taken over the canonical momentum distribution. The equation has a straightforward physical interpretation, acting to damp the difference between the instantaneous temperature corresponding to the component of relative velocity $\boldsymbol{v}_{ij}$ along the inter-particle vector, and the canonical ensemble average of this quantity. The prefactor Q_ξ controls the "thermal inertia" in the same way as the corresponding parameter in the conventional Nosé-Hoover method, and the function w gives a higher weighting to closer pairs. There is a conserved "energy function"

$$H_\xi(\boldsymbol{r},\boldsymbol{p},\xi,\varphi_\xi) = H(\boldsymbol{r},\boldsymbol{p}) + \tfrac{1}{2}Q_\xi\xi^2 + \varphi_\xi \qquad \text{where} \quad \dot{\varphi}_\xi = \xi k_{\rm B}T\sum_{i<j} w(r_{ij})^2/m_{ij} \tag{7}$$

as may be checked by time differentiation and direct substitution of the equations of motion.

3.2 *Integration Algorithm*

It is not the aim here to discuss the optimal algorithm for integration of the equations of motion (4). Instead, the simplest modified velocity-Verlet algorithm [19], that is commonly used in DPD [16], is adopted:

$$\tilde{\boldsymbol{p}}_i := \boldsymbol{p}_i := \boldsymbol{p}_i + \tfrac{1}{2}\Delta t\,(\boldsymbol{f}_i - \xi\boldsymbol{V}_i) \qquad \boldsymbol{p}_i(\tfrac{1}{2}\Delta t) \tag{8a}$$

$$\tilde{\xi} := \xi := \xi + \tfrac{1}{2}\Delta t\, G_\xi \qquad \xi(\tfrac{1}{2}\Delta t) \tag{8b}$$

$$\boldsymbol{r}_i := \boldsymbol{r}_i + \Delta t\,\boldsymbol{p}_i/m_i \qquad \boldsymbol{r}_i(\Delta t) \tag{8c}$$

$$\boldsymbol{f}_i := \boldsymbol{f}_i(\boldsymbol{r}) \qquad \boldsymbol{f}_i(\Delta t) \tag{8d}$$

$$\boldsymbol{V}_i := \boldsymbol{V}_i(\boldsymbol{r},\boldsymbol{p}) \qquad \boldsymbol{V}_i(\Delta t) \tag{8e}$$

$$G_\xi := G_\xi(\boldsymbol{r},\boldsymbol{p}) \qquad G_\xi(\Delta t) \tag{8f}$$

$$\boldsymbol{p}_i := \tilde{\boldsymbol{p}}_i + \tfrac{1}{2}\Delta t\,(\boldsymbol{f}_i - \xi\boldsymbol{V}_i) \qquad \boldsymbol{p}_i(\Delta t) \tag{8g}$$

$$\xi := \tilde{\xi} + \tfrac{1}{2}\Delta t\, G_\xi \qquad \xi(\Delta t) \tag{8h}$$

Steps (8e)–(8h) may be iterated to convergence, because the momenta at time $t+\Delta t$ should be used in the evaluation of G_ξ and $\boldsymbol{V}_i$. However, because of the expense of calculating the pairwise terms, in DPD it is usual to stop after one evaluation of the expressions above, and this is the approach adopted here. Some might prefer a strictly reversible integrator [20], while others favour the Runge-Kutta method: consideration of these possibilities is deferred.

3.3 *Configurational Nosé-Hoover Thermostat*

The canonical ensemble result

$$\sum_j \left\langle \left| \frac{\partial U}{\partial \boldsymbol{r}_j} \right|^2 \right\rangle = k_{\mathrm{B}} T \sum_j \left\langle \frac{\partial}{\partial \boldsymbol{r}_j} \cdot \frac{\partial U}{\partial \boldsymbol{r}_j} \right\rangle \,. \tag{9}$$

has been known for many years [21] and has recently been used to define a configurational temperature T_{c} in simulation [22, 23] and experiment [24, 25]. Recently, one of us [26] has suggested monitoring this quantity as an indicator of lack of equilibrium due to excessive timesteps in DPD. It is natural to consider applying a thermostat to control this variable [11, 27] and here the equations of motion of Braga and Travis [11] are used:

$$\dot{\boldsymbol{r}}_i = \boldsymbol{p}_i / m_i + \mu \boldsymbol{f}_i(\boldsymbol{r}) \tag{10a}$$

$$\dot{\boldsymbol{p}}_i = \boldsymbol{f}_i(\boldsymbol{r}) \tag{10b}$$

$$\dot{\mu} = G_\mu(\boldsymbol{r}) \tag{10c}$$

where

$$G_\mu = Q_\mu^{-1} \sum_j \left(\left| \frac{\partial U}{\partial \boldsymbol{r}_j} \right|^2 - k_{\mathrm{B}} T \frac{\partial}{\partial \boldsymbol{r}_j} \cdot \frac{\partial U}{\partial \boldsymbol{r}_j} \right) \,. \tag{11}$$

The quantity μ plays the role of a fluctuating mobility: that is, a proportionality between force and drift velocity, as seen in the "position Langevin equation" or Schmoluchowski equation [11]. Once again there is a conserved "energy function"

$$H_\mu(\boldsymbol{r}, \boldsymbol{p}, \mu, \varphi_\mu) = H(\boldsymbol{r}, \boldsymbol{p}) + \tfrac{1}{2} Q_\mu \mu^2 + \varphi_\mu \qquad \text{where} \quad \dot{\varphi}_\mu = \mu k_{\mathrm{B}} T \sum_j \frac{\partial}{\partial \boldsymbol{r}_j} \cdot \frac{\partial U}{\partial \boldsymbol{r}_j} \,. \tag{12}$$

Braga and Travis [11] have presented a simple integration algorithm for these equations, which is used here. The canonical distribution may also be shown to be a steady-state solution of the above equations of motion, and they share with the thermostatted equations of section 3.1 the property of Galilean invariance.

4 Results

Tests have been carried out using the standard "water" DPD model [28]: the potential strength parameter in eqn (2) was set to $\alpha = 25$, with simulation units defined so that $m = 1$, $k_{\mathrm{B}} T = 1$, $r_{\mathrm{c}} = 1$. A system of $N = 250$ particles was simulated in cubic periodic boundaries. Timesteps in the range $0.005 \leq \Delta t \leq 0.06$ were used, with run lengths up to 1000 reduced time units. For the pairwise Nosé-Hoover thermostat, inertia parameters in the range $0.2 \leq Q_\xi / N \leq 8.0$ were studied. For the configurational Nosé-Hoover thermostat, inertia parameters in the range $2000 \leq Q_\mu / N \leq 80000$ were used.

These thermostats allow one to check the accuracy of the integration by monitoring the conserved energy-function eqns (7) and (12). Figure 1 shows that, at timesteps $\Delta t > 0.02$ (very conservative by DPD standards), there is a significant drift in this quantity: the rate of increase is roughly proportional to Δt^4 at large Δt. This problem has been noted before by Hafskjold et al. [29], and it is not associated with the thermostatting, because the same behaviour is seen using the simple velocity Verlet algorithm. The cause seems to be the relatively strong discontinuity in force derivatives at the cutoff of the DPD potential [29]. In DPD, and in MD with a thermostat, this tends to be camouflaged. The present thermostats perform as well as (in fact, slightly better than) velocity Verlet in this respect.

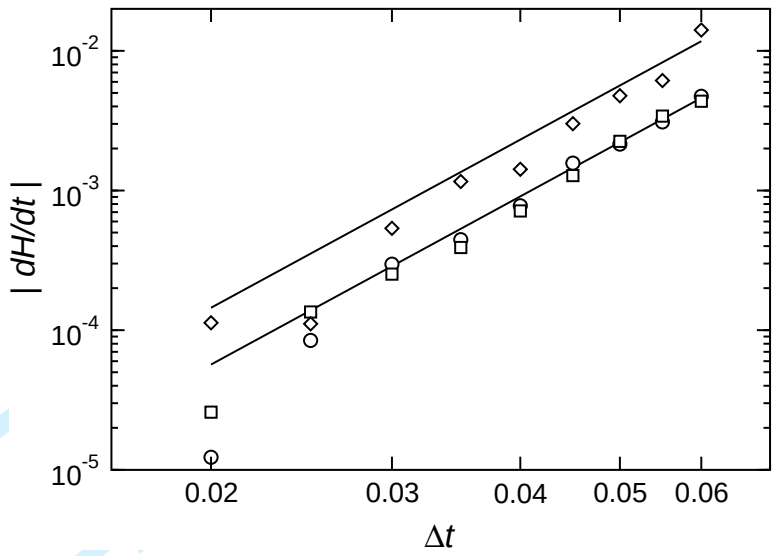

Figure 1. Rate of change of energy-like function as a function of timestep Δt, plotted on log-log scales. Circles: pairwise Nosé-Hoover thermostat with inertia parameter $Q_\xi/N = 0.8$. Squares: configurational Nosé-Hoover thermostat with inertia parameter $Q_\mu/N = 2 \times 10^4$. Diamonds: velocity Verlet algorithm, with no thermostatting. The lines correspond to Δt^4 power law behaviour.

The oscillation of the internal energy of the particles (potential plus kinetic) reflects the flow of energy into and out of the thermal reservoir, and this is influenced by the choice of thermal inertia parameter. Typical results are shown in Fig. 2, and they show the expected behaviour. There are damped oscillations: the runs lengths employed here are typically long compared with the relaxation rate, while the timesteps are small enough to cope with the oscillations. In this range, the precise choice of thermal inertia is not critical.

The simulation-averaged values of kinetic temperature T_k (defined through the total kinetic energy) and configurational temperature T_c (defined by eqn (9)) are shown in Fig. 3. When the kinetic temperature is controlled, lack of equilibrium is indicated by the configurational temperature, which increases by as much as 10% at the largest timesteps studied. These results simply confirm what has been seen before [26]: a measured kinetic temperature close to the desired value should not be taken as a guarantee that the system is at equilibrium. The form of the increase in T_c may be understood semi-quantitatively by considering the effect of non-zero-timestep velocity-Verlet dynamics on the phase portrait of a simple harmonic oscillator [26]. Conversely, when the configurational thermostat is imposed, the measured kinetic temperature is significantly reduced when the timestep is too large. This effect may be understood in a similar way by considering harmonic oscillator velocity-Verlet dynamics: for a given positional amplitude, the momentum amplitude is reduced as the timestep increases. When both thermostats are applied together, not surprisingly, both T_c and T_k are controlled well, up to the highest timesteps studied. This deserves further investigation, but it would be over-optimistic to suppose that the other degrees of freedom in the system are at equilibrium.

To illustrate the application to complex fluids, simulations of the same lipid bilayer model studied previously [26, 30, 31] have been carried out with the new thermostat. Here, the solvent water is represented as before, and each lipid molecule has the form of a 7-bead chain HT_6 in which α-repulsion parameters between hydrophilic "head" beads (H), hydrophobic "tail" beads (T), and "water" beads (W) are chosen to produce the desired behaviour [30]. Harmonic bond-stretching potentials, and angle-bending potentials, act within the lipid molecules. The measured temperatures of the different types of DPD bead are shown in Figure 4. The results are consistent with those obtained before [26] and show how dangerous it is to rely on thermostats to equilibrate the system when the timestep is too large: the different bead types have significantly different kinetic and configurational temperatures in all cases. Actually, for this simple model, the cause of the problem, and the remedy, are well understood. The *intramolecular* potentials within the lipid chains are too strong to be handled by the longer timesteps; this problem is easily addressed by using multiple timestep methods [32]. However, this example serves to illustrate possible pitfalls which may occur in the general case.

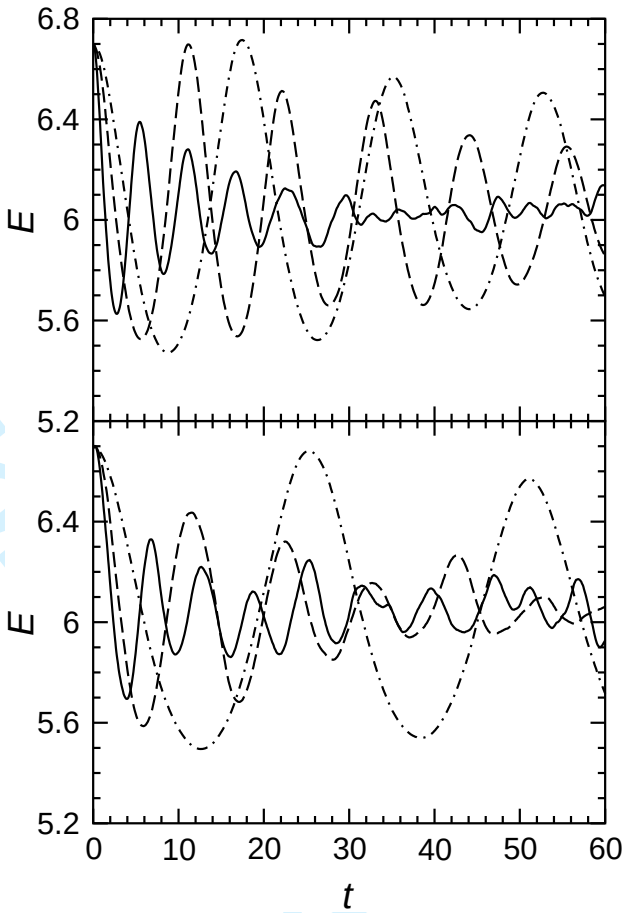

Figure 2. Oscillation of internal energy $E = H$ as a function of time t. Upper panel: pairwise Nosé-Hoover thermostat with inertia parameter: $Q_\xi/N = 0.2$ (solid line); $Q_\xi/N = 0.8$ (dashed line); $Q_\xi/N = 2.0$ (dot-dashed line. Lower panel: configurational Nosé-Hoover thermostat with inertia parameter: $Q_\mu/N = 8 \times 10^3$ (solid line); $Q_\mu/N = 2 \times 10^4$ (dashed line); $Q_\mu/N = 4 \times 10^4$ (dot-dashed line).

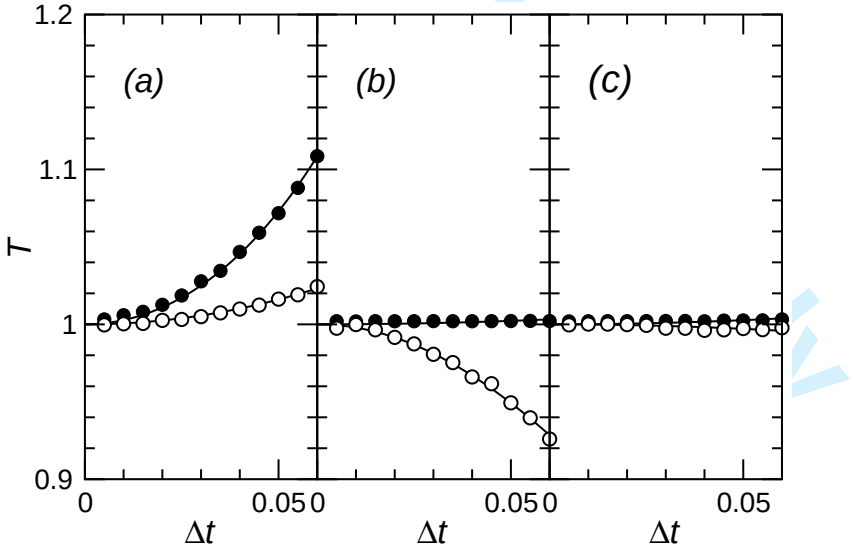

Figure 3. Kinetic temperature T_k (open symbols) and configurational temperature T_c (filled symbols) as functions of timestep Δt for three different thermostatting regimes: (a) pairwise Nosé-Hoover thermostat with inertia parameter $Q_\xi/N = 0.4$; (b) configurational Nosé-Hoover thermostat with inertia parameter $Q_\mu/N = 4 \times 10^3$; (c) both thermostats simultaneously.

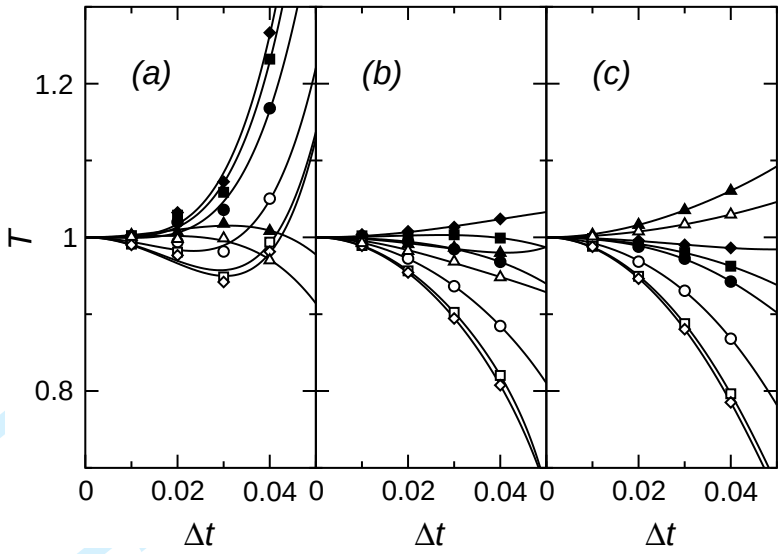

Figure 4. Kinetic temperature T_k (open symbols) and configurational temperature T_c (filled symbols) as functions of timestep Δt for membrane simulations using three different thermostatting regimes: (a) pairwise Nosé-Hoover thermostat with inertia parameter $Q_\xi/N = 0.4$; (b) configurational Nosé-Hoover thermostat with inertia parameter $Q_\mu/N = 4 \times 10^3$; (c) both thermostats simultaneously. Different symbols represent different DPD particle types: circles, H, T_6; squares, T_1, T_5; diamonds, T_2, T_3, T_4; triangles, water.

5 Discussion

The derivation of Section 3 establishes the canonical ensemble as a stationary distribution for the coordinates and momenta subject to the equations of motion (4), although it does not prove that it is unique, nor guarantee that a system will converge towards this distribution [5, 17, 18]. The result is easily generalized to apply to a subset of pair interactions, simply by setting $w_{ij} = 0$ for the omitted pairs, making this suitable to combine with the Lowe method as envisaged by Stoyanov and Groot [10]. (Interestingly, Ref. [5] contains exercises on incorporating a weighting factor, and on considering a subset of degrees of freedom, for the conventional Nosé-Hoover thermostat). Nosé-Hoover chains may easily be added to further control the dynamics [18].

The preliminary results presented above indicate that the pairwise Nosé-Hoover thermostat behaves as should be expected, and may be useful in both DPD and conventional MD / NEMD simulations. In simulations using DPD-like potentials, both this thermostat, and the configurational Nosé-Hoover thermostat of Braga and Travis [11], perform as well as other methods [26]; there are no problems, provided the timestep is not chosen too large.

A feature of the proposed thermostat, shared by the configurational-temperature thermostat, is the absence of peculiar velocities: this may provide a more satisfactory way of controlling the temperature than the conventional Nosé-Hoover thermostat in the case of fluid flows, since only local relative velocities are used to define an instantaneous temperature.

Acknowledgements

The comments of Brad Holian, Bill Hoover, and Karl Travis on an early version of the manuscript are gratefully acknowledged. This work was conducted while MPA was on Study Leave at the University of Bielefeld. The research has been supported by the Engineering and Physical Sciences Research Council, and by the Alexander von Humboldt foundation.

References

[1] S. Nosé. A molecular dynamics method for simulations in the canonical ensemble. *Molec. Phys.*, **52**, 255 (1984).

[2] S. Nosé. A unified formulation of the constant-temperature molecular dynamics methods. *J. Chem. Phys.*, **81**, 511 (1984).
[3] H. C. Andersen. Molecular dynamics simulations at constant pressure and/or temperature. *J. Chem. Phys.*, **72**, 2384 (1980).
[4] W. G. Hoover. Canonical dynamics - equilibrium phase-space distributions. *Phys. Rev. A*, **31**, 1695 (1985).
[5] W. G. Hoover. *Computational Statistical Mechanics*, volume 11 of *Studies in Modern Thermodynamics*. Elsevier (1991). ISBN 0-444-88192-1. Available online at `http://williamhoover.info/book.pdf`.
[6] J. Delhommelle, J. Petravic, D. J. Evans. On the effects of assuming flow profiles in nonequilibrium simulations. *J. Chem. Phys.*, **119**, 11005 (2003).
[7] D. J. Evans, G. P. Morriss. Shear thickening and turbulence in simple fluids. *Phys. Rev. Lett.*, **56**, 2172 (1986).
[8] D. J. Evans, S. T.Cui, H. J. M. Hanley, G. C. Straty. Conditions for the existence of a reentrant solid phase in a sheared atomic fluid. *Phys. Rev. A*, **46**, 6731 (1992).
[9] K. P. Travis, P. J. Daivis, D. J. Evans. Thermostats for molecular fluids undergoing shear flow: Application to liquid chlorine. *J. Chem. Phys.*, **103**, 10638 (1995).
[10] S. D. Stoyanov, R. D. Groot. From molecular dynamics to hydrodynamics: A novel Galilean invariant thermostat. *J. Chem. Phys.*, **122**, 114112 (2005).
[11] C. Braga, K. P. Travis. A configurational temperature Nosé-Hoover thermostat. *J. Chem. Phys.*, **123**, 134101/1 (2005).
[12] P. J. Hoogerbrugge, J. M. V. A. Koelman. Simulating microscopic hydrodynamic phenomena with dissipative particle dynamics. *Europhys. Lett.*, **19**, 155 (1992).
[13] J. M. V. A. Koelman, P. J. Hoogerbrugge. Dynamic simulations of hard-sphere suspensions under steady shear. *Europhys. Lett.*, **21**, 363 (1993).
[14] P. Espanol, P. Warren. Statistical mechanics of dissipative particle dynamics. *Europhys. Lett.*, **30**, 191 (1995).
[15] C. P. Lowe. An alternative approach to dissipative particle dynamics. *Europhys. Lett.*, **47**, 145 (1999).
[16] G. Besold, O. G. Mouritsen. Competition between domain growth and interfacial melting. *Comput. Mater. Sci.*, **18**, 225 (2000).
[17] D. Kusnezov, A. Bulgac, W. Bauer. Canonical ensembles from chaos. *Ann. Phys.*, **204**, 155 (1990).
[18] G. Martyna, M. L. Klein, M. Tuckerman. Nosé-Hoover chains: the canonical ensemble via continuous dynamics. *J. Chem. Phys.*, **97**, 2635 (1992).
[19] G. J. Martyna, D. J. Tobias, M. L. Klein. Constant-pressure molecular-dynamics algorithms. *J. Chem. Phys.*, **101**, 4177 (1994).
[20] G. J. Martyna, M. E. Tuckerman, D. J. Tobias, M. L. Klein. Explicit reversible integrators for extended systems dynamics. *Molec. Phys.*, **87**, 1117 (1996).
[21] J. O. Hirschfelder. Classical and quantum mechanical hypervirial theorems. *J. Chem. Phys.*, **33**, 1462 (1960).
[22] H. H. Rugh. Dynamical approach to temperature. *Phys. Rev. Lett.*, **78**, 772 (1997).
[23] B. D. Butler, G. Ayton, O. G. Jepps, D. J. Evans. Configurational temperature: Verification of Monte Carlo simulations. *J. Chem. Phys.*, **109**, 6519 (1998).
[24] Y. L. Han, D. G. Grier. Configurational temperature of charge-stabilized colloidal monolayers. *Phys. Rev. Lett.*, **92**, 148301 (2004).
[25] Y. L. Han, D. G. Grier. Configurational temperatures and interactions in charge-stabilized colloid. *J. Chem. Phys.*, **122**, 064907 (2005).
[26] M. P. Allen. Configurational temperature in membrane simulations using dissipative particle dynamics. *J. Phys. Chem. B*, **110**, 3823 (2006).
[27] J. Delhommelle, D. J. Evans. Configurational temperature thermostat for fluids undergoing shear flow: application to liquid chlorine. *Molec. Phys.*, **99**, 1825 (2001).
[28] R. D. Groot, P. B. Warren. Dissipative particle dynamics: Bridging the gap between atomistic and mesoscopic simulation. *J. Chem. Phys.*, **107**, 4423 (1997).

[29] B. Hafskjold, C. C. Liew, W. Shinoda. Can such long time steps really be used in dissipative particle dynamics simulations? *Molec. Simul.*, **30**, 879 (2004).

[30] J. C. Shillcock, R. Lipowsky. Equilibrium structure and lateral stress distribution of amphiphilic bilayers from dissipative particle dynamics simulations. *J. Chem. Phys.*, **117**, 5048 (2002).

[31] A. F. Jakobsen, O. G. Mouritsen, G. Besold. Artifacts in dynamical simulations of coarse-grained model lipid bilayers. *J. Chem. Phys.*, **122**, 204901 (2005).

[32] A. F. Jakobsen, G. Besold, O. G. Mouritsen. Multiple time step update schemes for dissipative particle dynamics. *J. Chem. Phys.*, **124**, 094104 (2006).

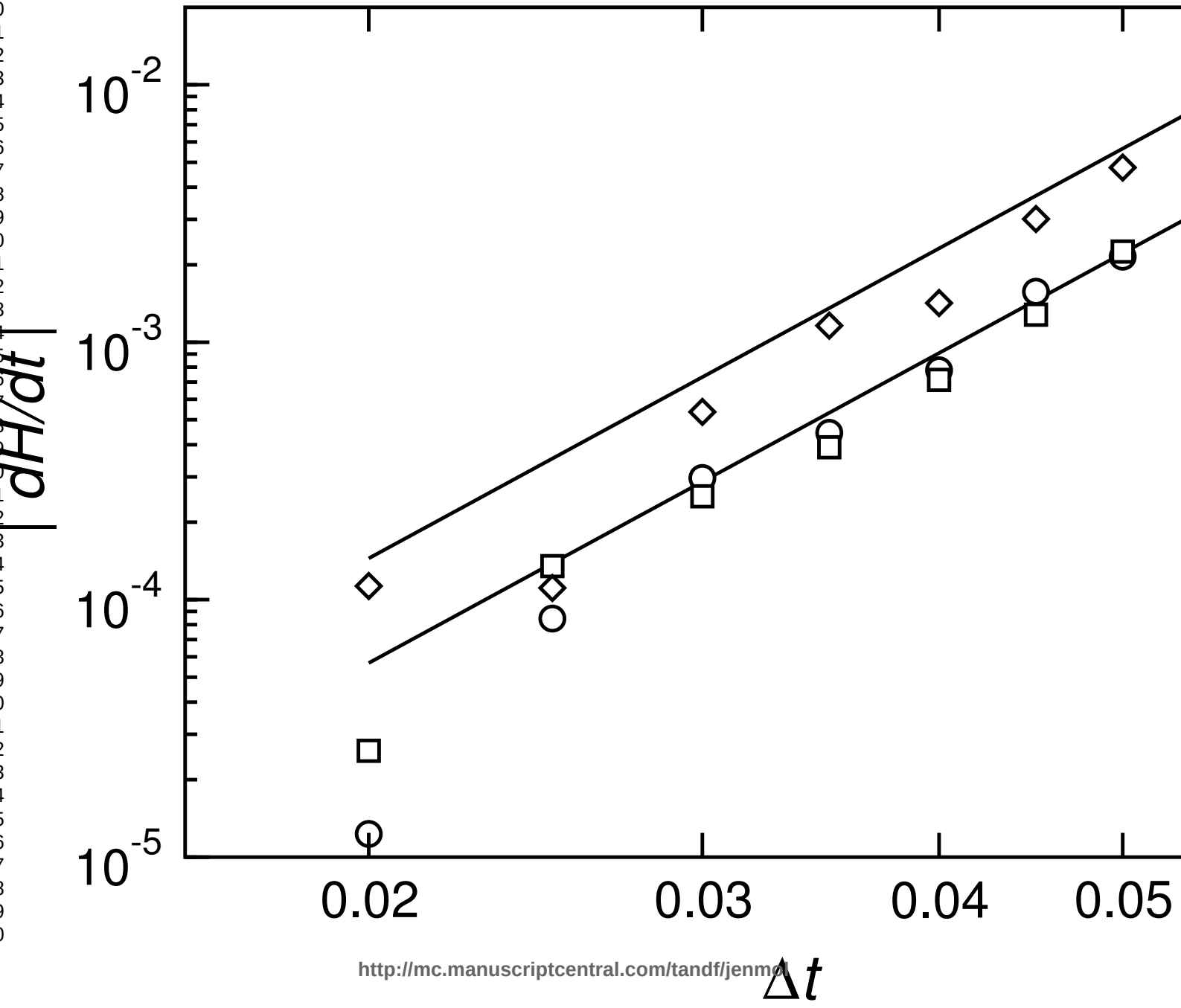
10^{-2}
10^{-3}
10^{-4}
10^{-5}
$|\,dH/dt\,|$
0.02
0.03
0.04
0.05
Δt

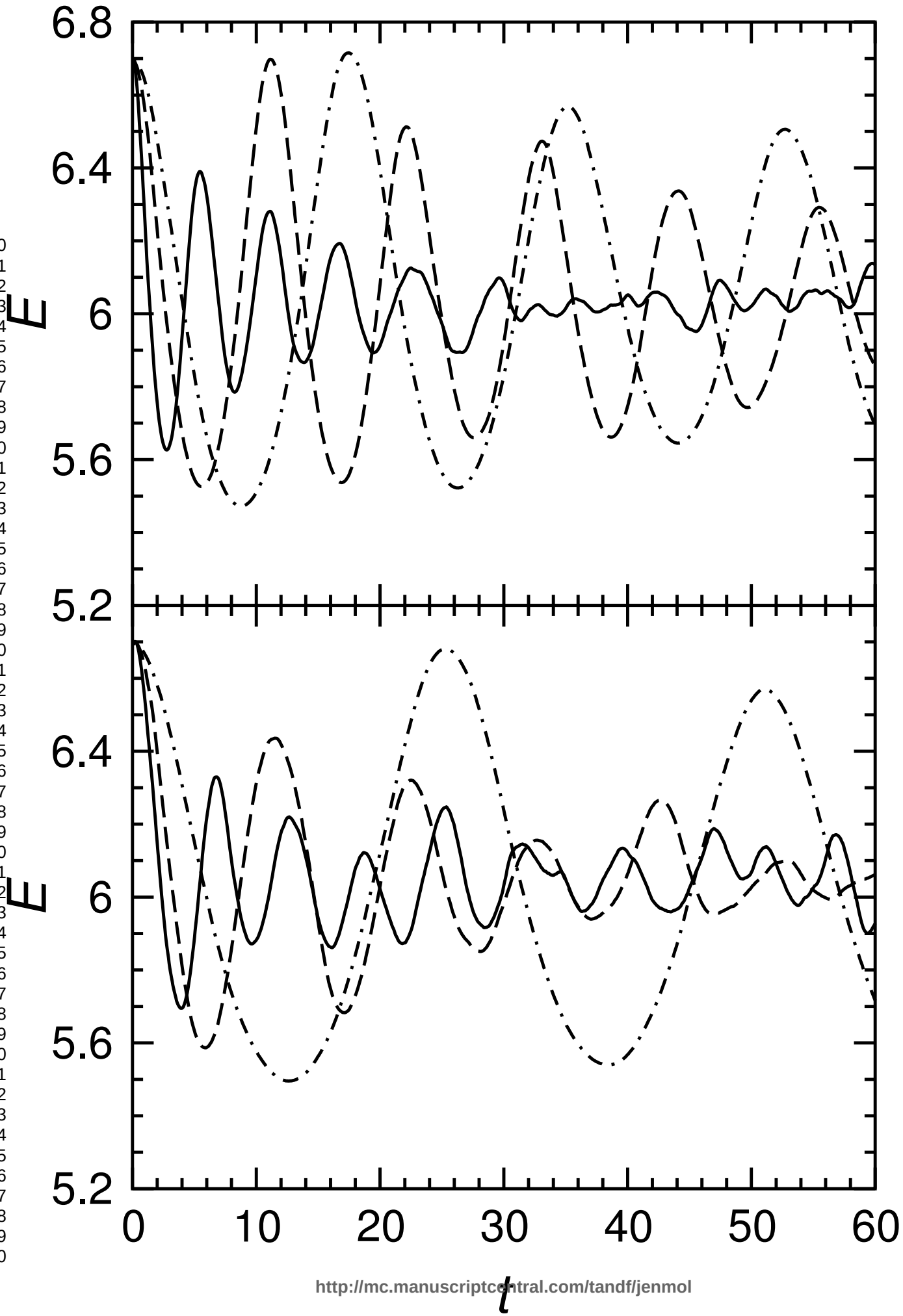
6.8
6.4
6
5.6
5.2
E
6.4
6
5.6
5.2
E
0
10
20
30
40
50
60
t

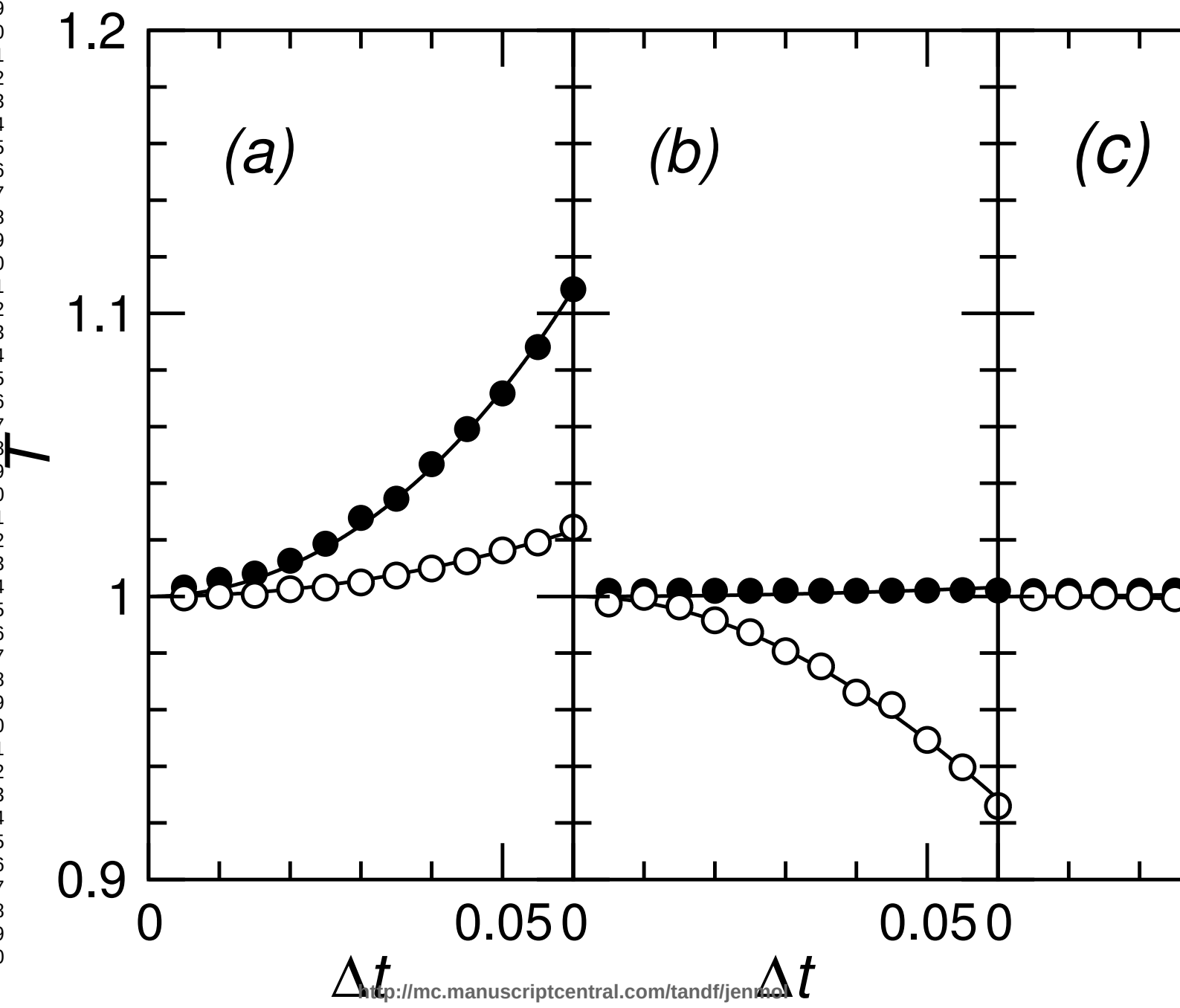
1.2
1.1
1
0.9
(a)
(b)
(c)
0
0.050
0.050
Δt
Δt

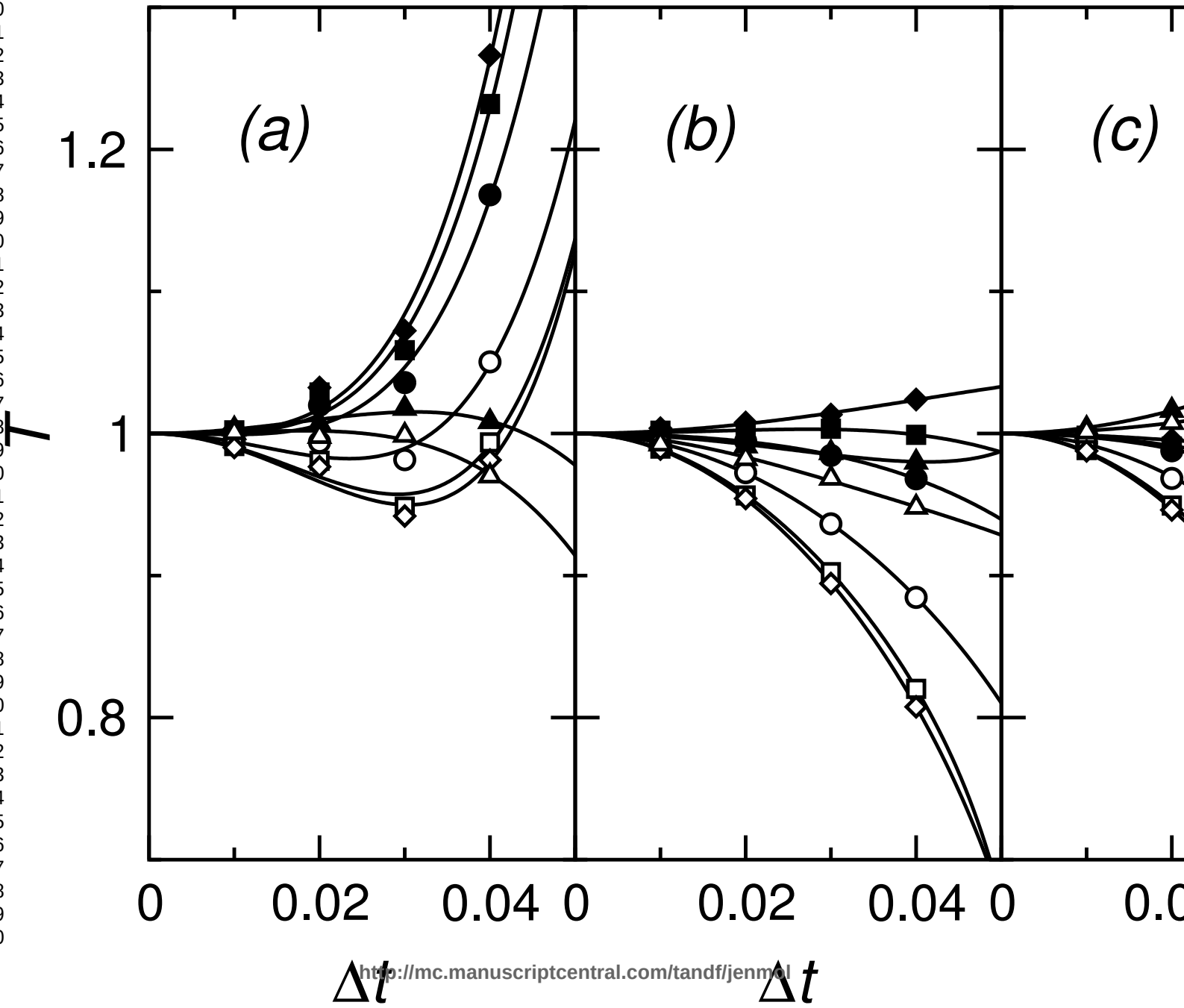
(a)
(b)
(c)
1.2
1
0.8
0
0.02
0.04
0
0.02
0.04
0
0.0
Δt
Δt